Field appraisal and accurate resource estimation from 3D quantitative interpretation of seismic and CSEM data

Jan Petter Morten, Friedrich Roth, and Stig Arne Karlsen, EMGS
David Timko and Constantin Pacurar, Fugro-Jason
Per Atle Olsen, Anh Kiet Nguyen, and Jakob Gjengedal, Statoil

The key questions in field appraisal are: What is the hydrocarbon volume, and how are the hydrocarbons distributed in the field? The ability to answer these questions accurately is critical for deciding whether to produce a field and for developing a production plan. Wells drilled during the appraisal phase provide well and flow-test data, which are combined with structural knowledge from seismic surveys to map the extent of the field and generate a reservoir model. The cost for appraising an offshore field can exceed US $100 million, and it is desirable to obtain the information required with fewer wells if possible. Quantitative interpretation of surface geophysical data provides reservoir properties between well locations and can, therefore, significantly reduce appraisal costs.

A quantitative analysis of seismic data using well-log information will typically determine reservoir rock porosity. Other important parameters are hydrocarbon saturation, permeability, and net-to-gross ratio. Quantitative interpretation of several reservoir properties using only the seismic data is associated with significant ambiguity. To determine several of these parameters accurately, complementary geophysical data sets with different sensitivity characteristics are needed. Controlled-source electromagnetic (CSEM) data are sensitive to the fluid type and can provide additional information to determine the hydrocarbon saturation more accurately.

We have developed a new quantitative interpretation workflow integrating seismic and marine 3D CSEM data for estimating the hydrocarbon volume and obtaining 3D distributions of the hydrocarbon pore volume. A performance test of the workflow has been carried out on the Troll West Oil Province (TWOP) in the Norwegian North Sea (Figures 1 and 2). This article describes our methodology and presents encouraging results.

After correction for systematic errors, our predictions deviate by only a few percent from corresponding quantities derived from the reservoir simulation model. The simulation model incorporates accumulated knowledge of the Troll Field from an extensive database, including all well logs, produc-

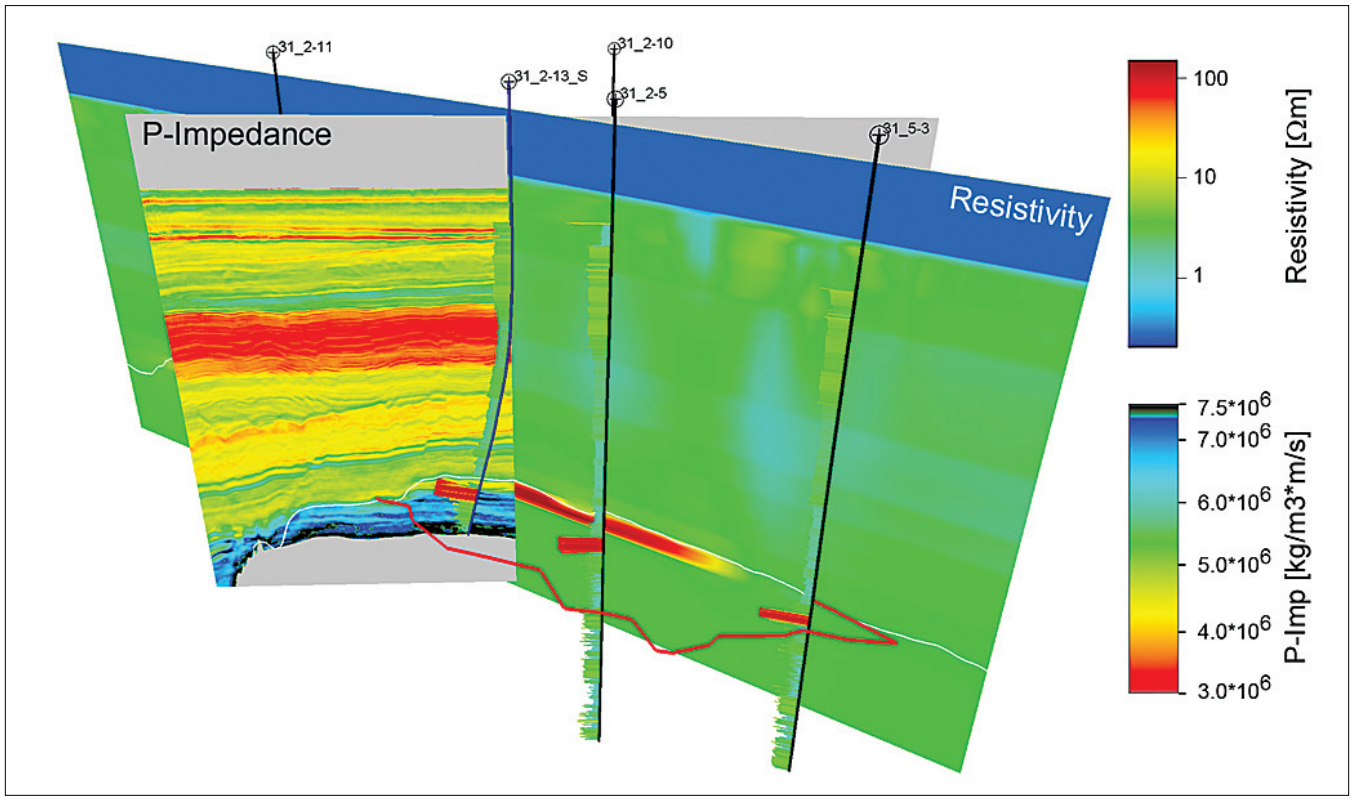

Figure 1. *3D view of the Troll West Oil Province showing well positions, resistivity tracks, the field outline (red polygon), and vertical sections from inverted P-impedance and vertical resistivity volumes. The geophysical parameters can be used to determine reservoir properties such as hydrocarbon saturation and effective porosity in a joint quantitative interpretation workflow.*

tion data, and time-lapse seismic data. Furthermore, our volume predictions are significantly more accurate than those obtained by extrapolation of saturation profiles interpreted from exploration well logs. The lateral variations in the hydrocarbon saturation also correlate well with the expected production effects of injection and depletion (Figure 3a).

The joint quantitative interpretation study of the TWOP is complemented by a thorough uncertainty analysis, and we describe how to estimate the systematic errors and provide bounds on computed values. The volumetric and spatial agreement with the reservoir simulation model establishes the study as a proof-of-principle case for the presented methodology.

Seeing between wells

Well data have limited resolution away from the borehole, so several wells may be required to delineate a reservoir with a complicated shape and internal sealing structures. Surface geophysical data such as 3D seismic and 3D CSEM will provide continuous lateral coverage but with less vertical resolution. An approach where well measurements are complemented by surface data may provide sufficient information for appraisal and resource estimation with fewer wells. In this case, the wealth of physical parameters measured in the well can be used to establish quantitative rock physics models or empirical relationships. Such models describe how the geophysical parameters such as the P-impedance and the V_P/V_S ratio for seismic data and the vertical resistivity for CSEM data are related to reservoir properties. By inverting the surface data and applying the models to the resulting geophysical parameters, spatial variation of reservoir properties can be determined quantitatively.

One of the most important reservoir properties estimated during field appraisal is the hydrocarbon pore volume. The distribution of the hydrocarbon pore volume depends on several reservoir properties, and therefore quantitative interpretation requires several independent physical measurements. Prestack seismic data are typically sensitive to porosity and can also give information about net pay thickness and fluid type if the conditions are favorable. The CSEM data are sensitive to the hydrocarbon saturation, but can also be influenced by porosity and clay content. In some reservoirs, not all reservoir properties exhibit considerable variations, such that simplifying assumptions can be made and interdependencies do not need to be considered explicitly. In the reservoir characterization we consider in this article, the exploration well logs showed that the clay content of the reservoir rock is low. Therefore, the presence of clay could be treated as a perturbation to the rock physics model. The reservoir characterization thus required us to determine the porosity and the hydrocarbon saturation to which seismic poststack data and CSEM data respectively are sensitive.

Previous studies in which seismic and CSEM data are jointly interpreted (Hoversten et al., 2006; Harris et al., 2009; Dell'Aversana et al., 2011) have shown that quantitative information on reservoir porosity and water saturation can be predicted. The input data and interpretation workflows of these published studies have until now been limited to 2D profiling. However, to be directly relevant to resource estimation and field appraisal, the full 3D variations in the reservoir properties must be determined. This facilitates volumetric computations and lateral definition of the fluid distributions. Moreover, quantitative determination of the hydrocarbon saturation for reservoirs with a lateral size smaller than 4 km requires that 3D effects are taken into account during both acquisition and interpretation, even along 2D profiles (Morten et al., 2011). In this article, we show how 3D seismic and 3D CSEM data can determine the lateral variations in reservoir properties.

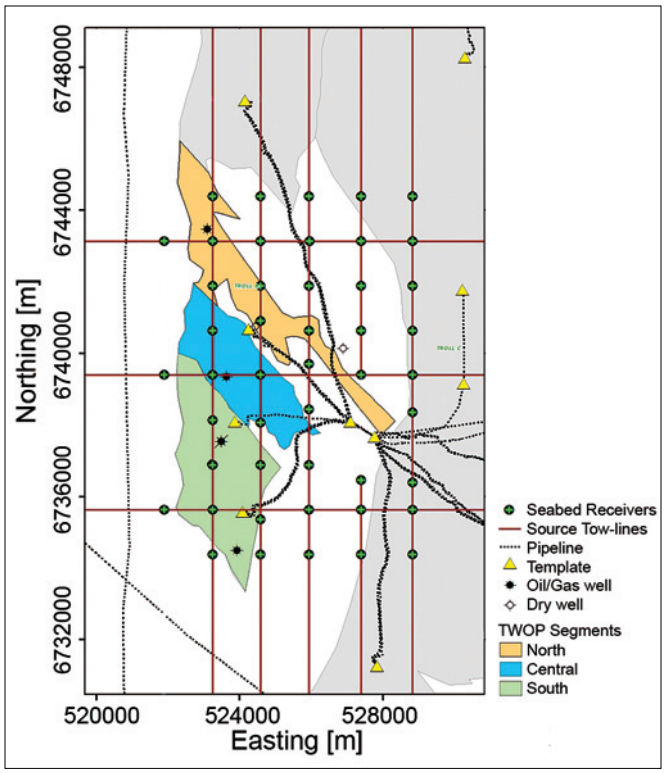

Figure 2. *Map view of the Troll West Oil Province showing the production infrastructure and CSEM survey layout.*

Troll West Oil Province

The Troll Field is the biggest gas field in the North Sea but it also has significant quantities of oil in thin zones under the gas cap. The field has been producing since 1995 (Mikkelsen et al., 2005). Troll extends over three fault blocks tilted east, and is subdivided into Troll East, Troll West Gas Province (TWGP), and Troll West Oil Province (TWOP). In this study, we focus on the TWOP (Figure 2) which is a smaller (25 km^2) segment of the reservoir where the oil column is thicker (15–27 m). The oil is produced from horizontal wells placed close to the oil–water contact. The main drive mechanism is gas cap expansion, with pressure support from one gas injector. The reservoir sediments are part of the Upper Jurassic Sognefjord Formation and consist of layers of clean medium-to-coarse grained, high-permeability sand, micaceous fine-grained sand, and siltstone with low-to-medium

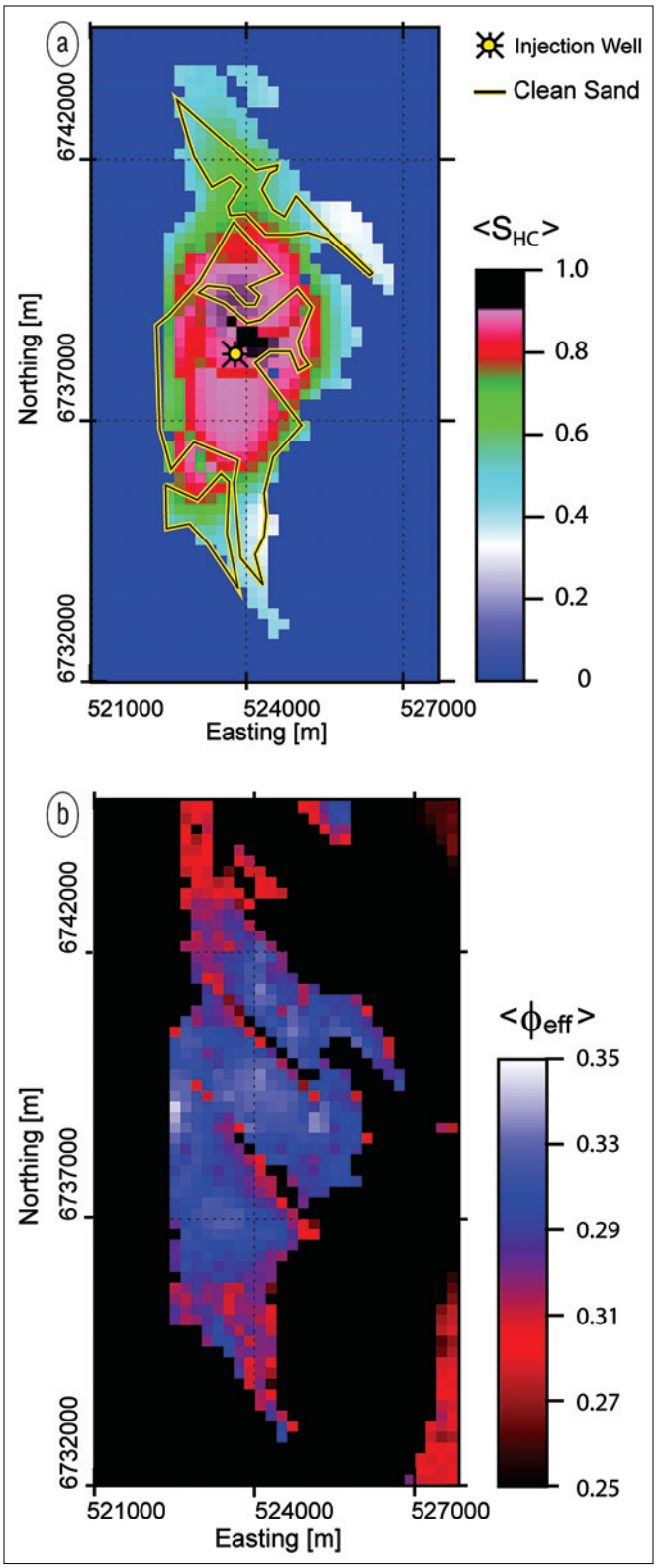

Figure 3. *Troll West Oil Province: (a) hydrocarbon saturation, $S_{HC} = 1 - S_w$, and (b) effective porosity, ϕ_{eff}, averaged in depth over the hydrocarbon zone. In (a), the central part close to the indicated gas injection well, 31/2-B-3, is mapped with anomalously high S_{HC}. The black-yellow polygons show regions at the original gas-oil contact level where the reservoir sands exhibit predominantly high permeability. The expected water intrusion pattern for the southeastern edge of the field correlates with a small area mapped with low S_{HC}.*

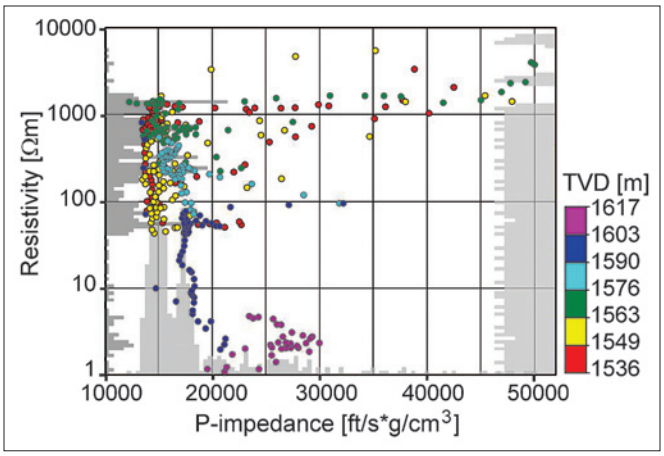

Figure 4. *Crossplot of P-impedance against resistivity from well-log data in the reservoir interval. The correlation between these quantities is weak (i.e., for a given P-impedance, the resistivity can take a wide range of values and vice versa).*

permeability. The sediments were deposited in a shallow marine environment influenced by tidal and fluvial processes.

The TWOP quantitative interpretation study was performed as a blind test. The hydrocarbon pore volume distribution and total hydrocarbon volume were predicted and then compared with established reserves data. To simulate an appraisal phase of development, we used only logs from the exploration wells that were drilled during 1984–85. For the TWOP, 3D seismic data are repeatedly acquired, and we used poststack data from the 2003 survey. The well and seismic data are publicly available from the Norwegian Petroleum Directorate. Additionally, we used data from a 3D CSEM survey acquired in 2008 as part of an R&D collaboration between Statoil and EMGS (Gabrielsen et al., 2009).

The restrictions on input data were limiting factors for the quantitative interpretation. Specifically, the well data did not include shear-wave velocity and the publicly available seismic information consisted of poststack data. This limited the seismic inversion to the estimation of P-impedance; nevertheless, the good results obtained indicate that the P-impedance captures the most important reservoir information for the TWOP. Finally, production infrastructure prohibited complete CSEM coverage over the field and also induced noise in the CSEM data.

Petrophysical analysis

High-quality seismic reservoir characterization requires well-log data that are consistent between formations and wells, cover the entire vertical interval of interest, and represent the true, undisturbed rock properties. The well data used in this study were quality controlled for these criteria, and corrections were applied where necessary.

The shale, clean sand, and sand-clay trends were then determined and used in the petrophysical analysis to estimate clay volume, porosity, and water-saturation parameters. The shear sonic log was missing from the input data, and therefore rock physics modeling was used to synthesize these data from the P-sonic log using the Greenberg-Castagna empirical rela-

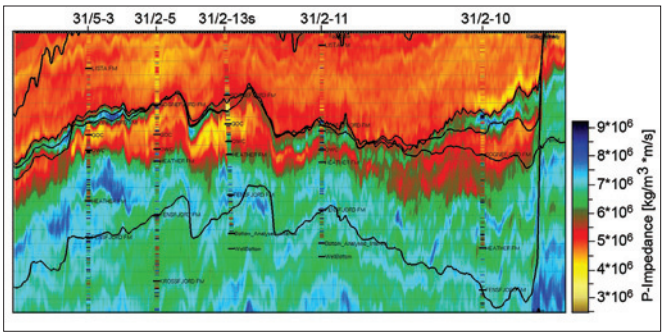

Figure 5. *Display of inverted P-impedance. Vertical profile display of inverted P-impedance. The vertical section intersects the well positions, and the P-impedance observed in the wells is superposed.*

tionship. This modeling study showed that a linear trend can approximate the relationship between P- and S-impedance. However, the trend is different for gas-saturated sandstones compared to the lithotypes shale, and oil- or brine-saturated sandstones.

To estimate the effect of hydrocarbon saturation on the logged resistivity, we found suitable parameters for the Simandoux resistivity model to consistently describe the well data. We then carried out a fluid substitution analysis, which showed a significant increase in resistivity when the hydrocarbon saturation is higher than 45%.

Seismic and CSEM inversion

The aim of the joint interpretation of seismic and CSEM data is to obtain a subsurface model that consistently describes both these measurements. We conducted independent seismic and CSEM inversions to obtain such a model, as the correlation between the reservoir P-impedance and the resistivity is weak (Figure 4). The CSEM data have lower spatial resolution than the seismic data owing to the lower signal frequencies involved. To preserve the fine-scale structural information available in the seismic interpretation, we imposed a geometry-based regularization constraint in the CSEM inversion.

A seismic inversion for P-impedance was carried out on the poststack data using the InverTrace algorithm in the Jason Geoscience Workbench software. A vertical section intersecting the well positions is shown in Figure 5. A low-frequency P-impedance model is required to constrain the inversion. This model was created using the well information from the public domain and a velocity model and depth surfaces provided by Statoil. After the initial inversion, adjustments were made to the surfaces in time and to the velocity model to facilitate more accurate translation of the inverted P-impedance and associated reservoir property volumes to the depth domain.

The anisotropic 3D CSEM inversion is described in Zach et al. (2008). The seismic top reservoir horizon and the oil–water contact observed in the exploration wells determined the structural constraint for the hydrocarbon zone of the reservoir. Using this information, regularization was formulated to favor a typical formation resistivity in the background and allow for an anomalously high-resistivity inside the hydrocarbon-saturated part of the reservoir. The final 3D inversion model generally fits the observed data to within the estimated data uncertainty. No well data were explicitly used in the CSEM inversion, and therefore the resistivity logs for the overburden could be used to quantitatively assess the accuracy of the inverted horizontal resistivity model.

Figure 6 shows that the resistivity correspondence is good and that the background resistivity trends are correctly predicted. The subsea infrastructure appears as a conductive artifact spatially separated from the hydrocarbon reservoir. Note that the vertical resistivity was not measured in the well and a comparison of this component was therefore not possible.

Joint quantitative interpretation

Quantitative prediction of reservoir properties is possible if we can establish accurate cross-property relationships to the geophysical parameters obtained from inversion (namely the P-impedance and the vertical resistivity). We used the exploration well-log data to establish such cross-property relationships. The well data have different measurement scales compared to seismic and CSEM data. Therefore, it was necessary to upscale the well data to the appropriate length scales prior to the correlation.

As seismic data are often sensitive to porosity, we considered the crossplot of P-impedance and effective porosity. Figure 7a shows that the impedance associated with the hydrocarbon-charged reservoir zone has a reasonable correlation with effective porosity, which is fitted by the trend line shown. The gas- and oil-saturated zones would be fitted better with separate trends as can be expected from the difference observed in the petrophysical modeling. We will explore the effect of this further in the error analysis below. The data from the brine-saturated reservoir zone show more scatter, which is consistent with the higher abundance of clay observed in the well logs. The clay volume is an additional parameter that should be determined if the relationship was to be used for this part of the reservoir.

In addition to the logged horizontal resistivity, supplemental information about the electrical anisotropy at the well-log scale is generally required to predict the anisotropic resistivity at the CSEM scale. From log analysis of several deviated wells in the North Sea, Ellis et al. (2010) found that the relationship between horizontal and vertical resistivity depends on the lithology. They concluded that North Sea sandstones typically have similar horizontal and vertical resistivities at the well-log scale (i.e., they are close to isotropic). However, anisotropy still arises in the upscaled well data owing to bedding and needs to be considered when establishing cross-property relationships for resistivity at the CSEM scale.

The upscaled water saturation was computed by averaging over the pore volume described by the effective porosity. Figure 7b shows the well data and a fit to the Simandoux rock physics model, which can be expressed as

$$\frac{1}{R} = a\,(S_w)^n + c,$$

Reservoir segment	HC volume deviation, %
North	–29.1
Central	–2.9
South	–7.6
Total	**–11.6**

Table 1. *Troll West Oil Province hydrocarbon volume deviation between reservoir simulation model as of 1 July 2008 and the prediction from the quantitative interpretation results. The volume deviation is particularly large in the northern reservoir segment, where the reservoir is thin and seismic resolution becomes an issue.*

where R is the resistivity, S_w is the water saturation, and a, n, and c are fitting parameters. The parameter c provides corrections for clay. Beds with high resistivity will dominate the vertical resistivity at the CSEM scale. Therefore, the upscaled data concentrate on higher resistivity values. The brine-saturated zone associated with lower resistivity gives rise to a cluster of points at high water saturation, thus resulting in a well constrained rock physics model.

The established cross-property relationships enabled us to predict the effective porosity and the water saturation from the seismic and CSEM inversion results. The results are shown in Figure 3a and 3b for water saturation and effective porosity, respectively.

Resource estimation and comparison with production reservoir model

The results for water saturation, S_w, and effective porosity, ϕ_{eff}, can be combined to predict hydrocarbon volume (i.e., resource estimation). The hydrocarbon pore volume (HCPV) at a position $\mathbf{r}$ is determined by

$$\mathrm{HCPV}(\mathbf{r})=(1-S_w(\mathbf{r}))\phi_{\mathrm{eff}}(\mathbf{r}).$$

Integrating this quantity in depth over the reservoir interval gives the hydrocarbon pore column (HCPC) map, which is shown in Figure 8. As this quantity strongly correlates to reservoir thickness, the intrareservoir variations are more clearly demonstrated in, for example, the water-saturation map of Figure 3a. When resource estimation is performed using well data alone and not by quantitative interpretation, only the points where wells penetrate the reservoir will be known on this map. The accuracy of the resource estimation will then depend on the quality of the interpolation and extrapolation from these points.

Hydrocarbon volume estimates are obtained by integrating the hydrocarbon pore volume over the volume of interest. We compared the volumes predicted from the quantitative interpretation with the volumes from the historical Troll reservoir simulation model for the time when the CSEM data were acquired. The comparison of hydrocarbon volumes was carried out for three reservoir segments (see Figure 2) and the results are summarized in Table 1. The total deviation in hydrocarbon volume is –11.6% (i.e., the volume was underestimated in the quantitative interpretation). Below, we show that two of the largest sources of error are systematic and can be partly compensated for. Utilizing these corrections, the prediction agrees with the volumes derived from the reservoir simulation model. The error propagation analysis showed that the expected uncertainty is ±10%.

To demonstrate the accuracy of the hydrocarbon volume prediction from the joint quantitative interpretation given the limited input data, we considered a more conventional resource estimation in which CSEM data were not utilized. We still assumed that the porosity distribution is determined through seismic inversion in the way described above. The hydrocarbon saturation was, instead, determined by interpolating well data. As the exploration well logs utilized in this study were acquired before production started, this result is biased when compared to the numbers in Table 1. However, we believe the results are still relevant because production is from the zone close to the oil–water contact and is driven by gas cap expansion. The resulting deviation from the reservoir simulation model is +18.4%. Applying the same correction for systematic errors in the porosity as used in the quantitative interpretation workflow, the result is more than +20% off. This demonstrates the potential for more accurate resource estimation when CSEM is utilized.

Hydrocarbon distribution

Let us consider the correlation between the predicted hydrocarbon saturation distribution, and the expected effects resulting from gas injection. There is a fault between the central and southern reservoir segments (see Figure 2). The fault zone is likely to be associated with reduced permeability. Figure 3a shows a region of lower hydrocarbon saturation that correlates well with the fault strike direction. That could be due to less efficient gas injection into this zone. Close to the gas injection site, we can expect anomalously high hydrocarbon saturation. Figure 7b shows that even small increases in hydrocarbon saturation at the high saturation end can considerably increase the local resistivity and be measured using CSEM data. The hydrocarbon saturation map, Figure 3a, indicates the surface position of the injection well. The position of the gas injection correlates well with the predicted zone of anomalously high hydrocarbon saturation.

Owing to production, water intrusion at the edges of the TWOP can be expected. However, the degree of oil substitution by water will depend on reservoir permeability. In areas with highly permeable sands, drainage occurs more efficiently and more water intrusion should result. The saturation map, Figure 3a, shows a local zone of reduced hydrocarbon satura-

Type of error	Influence on predicted hydrocarbon volume, %
Tuning effects (systematic)	–7.6
Underestimated reservoir resistivity (systematic)	–5
Inaccurate trend P-impedance to porosity	±7.5
Discretization	±4.3
Rock physics model parameters	±4

Table 2. *Results of the error propagation analysis.*

tion in the southeast. Spatially, this region correlates to an area where there is more highly permeable sand, as indicated by the polygon.

Error analysis

We performed an extensive error propagation study to determine the uncertainty bounds on the hydrocarbon volume predictions and to identify the main sources of error in the study. Two large identified contributions are systematic errors. The contributions to the uncertainty are summarized in Table 2.

The data in Table 1 show that the discrepancy in the predicted hydrocarbon volume is large in the northern reservoir segment. This segment is anomalous in the sense that the sand layers are typically thinner than in the central and southern segments. We investigated whether this would introduce errors related to seismic resolution. From the wavelet spectrogram and the velocity model, the length scale for tuning effects was estimated to be 15 m, a thickness also observed for sand intervals identified from well logs in the northern segment. The expected effect on the seismic inversion result is that the impedance would be smeared vertically, and thus the porosity of the sand layers would be underestimated. Typically, there is a compensating effect in that the layer thickness is overestimated, but in this study the reservoir thickness was defined independently by the top reservoir horizon and the oil–water contact.

We applied a correction to the porosity volumes to estimate the magnitude of the error and obtain a more accurate porosity for the given structural model. Where the reservoir thickness, t, is less than 15 m, we scaled the porosity up by the factor of $15/t$. An upper limit for the porosity based on the maximum value observed in the thicker reservoir segments was applied. When we recalculated the total hydrocarbon volume using the corrected effective porosity model, we obtained a 7.6% larger value.

The water-saturation model was determined from the 3D CSEM inversion resistivity. The inversion was run with an initial model that did not incorporate a resistive anomaly associated with the presence of hydrocarbons. The resistivity in the reservoir zone was iteratively increased by the inversion to reduce the discrepancy between the field and modelled data. This process converged when the residual response due to the resistivity difference between the inversion model and the actual reservoir resistivity fell below the measurement accuracy and, hence, that remaining difference could not be resolved. Therefore, we expect the resistivity to be underestimated by the inversion. We performed a modeling study and found that an increase in reservoir resistivity of up to 10% in the final inversion model does not induce a significant increase in data misfit. This increase in resistivity introduces a smaller, 5%, increase in hydrocarbon saturation, as the water saturation changes slowly with increasing resistivity when a high reservoir resistivity is reached (Figure 7b).

The relationship between effective porosity and P-impedance was determined by fitting a trend line to the upscaled

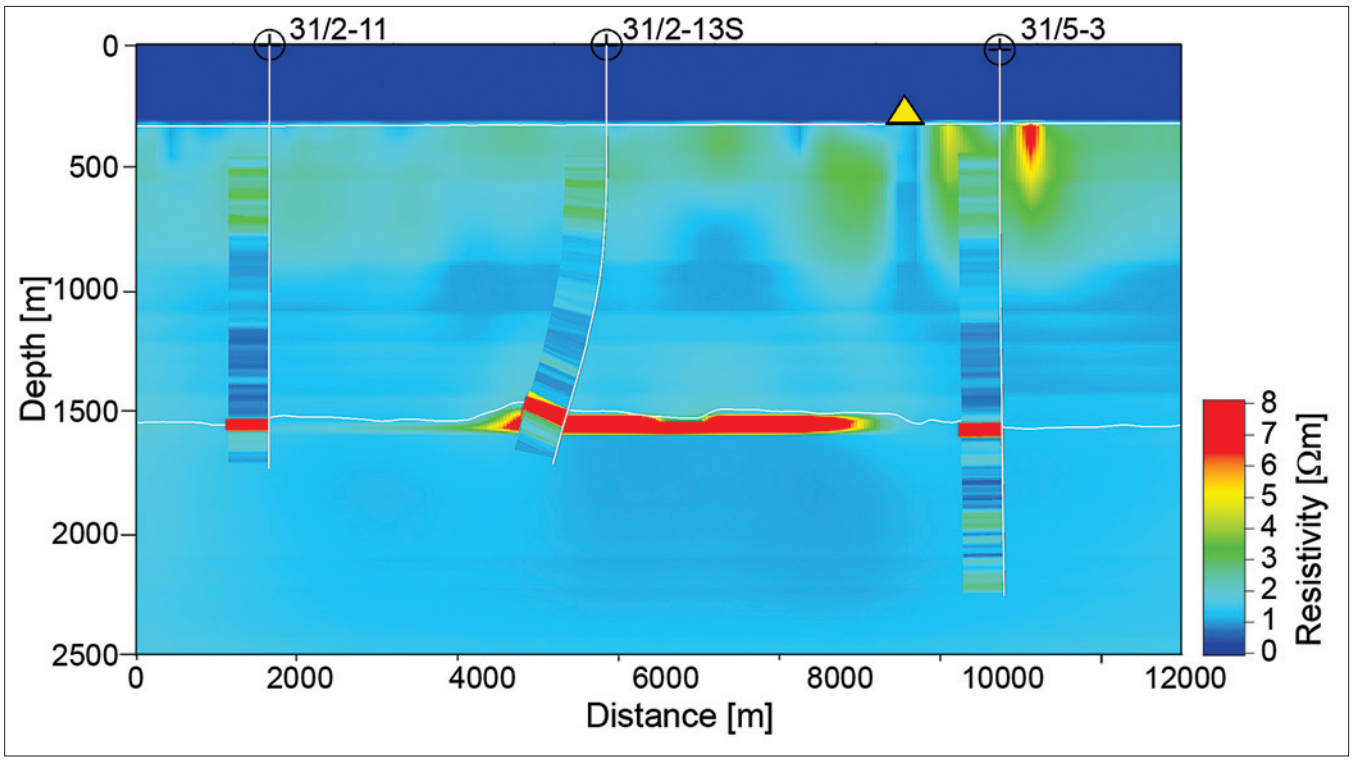

Figure 6. *Horizontal resistivity model from the anisotropic 3D CSEM inversion with well tie. The vertical section intersects well positions 31/5-3, 31/2-13S, and 31/2-11. The yellow triangle marks the position of the subsea installation cluster leading to a conductive anomaly in the inverted model. The horizontal resistivity model has limited sensitivity to the thin, hydrocarbon reservoir resistive anomaly, which explains the apparent discrepancies at 31/2-11 and 31/5-3.*

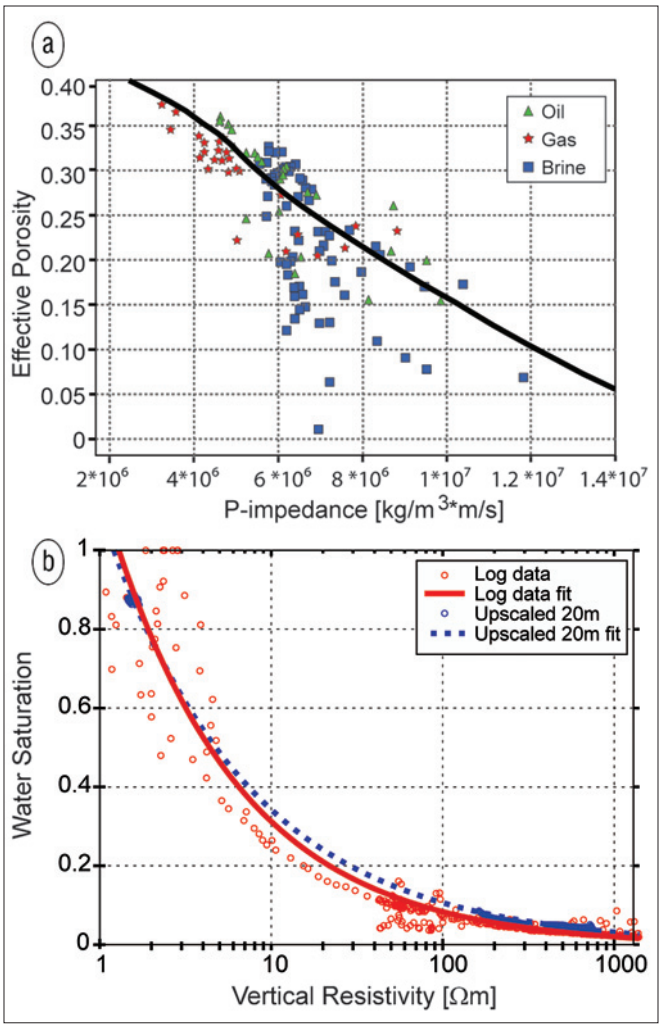

Figure 7. *Crossplots from upscaled well data in the reservoir interval. The relationships are used to determine the reservoir properties from inverted volumes of (a) P-impedance and (b) vertical resistivity.*

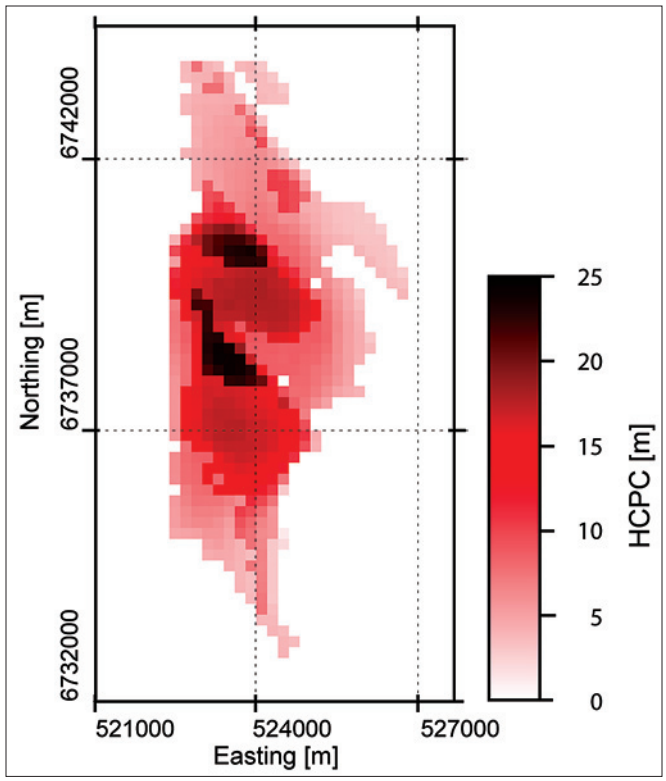

Figure 8. *Hydrocarbon pore column HCPC=$\int_{Reservoir}$ HCPV dz in meters.*

well data (Figure 7a). The input data include measurements from both gas- and oil-saturated reservoir zones. Due to the density variation between these two phases, slightly different trends can be expected when constructing these relationships separately for data from either the gas or oil zone. It is not possible to apply these separate trends directly, as the phases are not separated owing to the nonequilibrium reservoir state from production and injection. An average trend is more likely to give an accurate result. However, to estimate the variation in hydrocarbon volume prediction associated with different trends, we calculated that the hydrocarbon volume change is ±7.5% when applying trends based on data from either the gas or the oil zones identified in the exploration logs.

The rock physics model parameters used when interpreting the water saturation from well data were treated as fitting parameters, and we investigated the uncertainty in hydrocarbon volume prediction due to uncertainty in these parameters. We used the Simandoux resistivity model and considered errors in tortuosity factor, brine resistivity, and saturation and cementation exponents. This study was performed by making 10% changes to the parameters and then calculating the resulting change in hydrocarbon volume. Typically, we found that the associated volume change is ±4% or smaller, which indicates the magnitude of uncertainty associated with such errors.

The CSEM inversion utilized a coarse model discretization consistent with the expected resolution for the low frequencies involved. We investigated the error from this discretization and estimated that the total hydrocarbon volume error is less than 3%.

Another discretization effect that can influence the hydrocarbon volume prediction is small-scale deviations from a flat oil–water contact. This uncertainty is difficult to quantify, as the actual fluid contact may not be well defined because of drainage, injection, fingering, and nonequilibrium effects. The net water line will probably rise to the level of the horizontal production wells over time. If the actual oil–water contact is effectively 2 m above the level used in the inversion constraint over the whole TWOP, the hydrocarbon volume prediction will be 4.3% too large.

Conclusion and outlook

We have applied a new methodology for joint quantitative interpretation of 3D CSEM and seismic using data from the TWOP. The accuracy of the resource estimate and the resolution of the spatial details in the hydrocarbon saturation establish our study as a proof-of-principle case for future applications in field appraisal. Moreover, the results demonstrate the potential to extract large-scale information about hydrocarbon-saturation variations that are caused by field production. We also considered uncertainty in the predic-

tions, and quantified how our workflow increases accuracy compared to the case without CSEM data. The input data set was representative of the information available in an appraisal setting. We believe that the type of information achieved in this study could be valuable in resource estimation, delineation, and planning of further appraisal wells. TLE

References

Dell'Aversana, P., S. Carbonara, S. Vitale, M. A. Subhani, and J. Otiocha, 2011, Quantitative estimation of oil saturation from marine CSEM data: a case history: First Break, **29**, no. 2, 53–62 .

Ellis, M., M. Sinha, and R. Parr, 2010, Role of fine-scale layering and grain alignment in the electrical anisotropy of marine sediments: First Break, **28**, no. 9, 49–57.

Gabrielsen, P. T., I. Brevik, R. Mittet, and L. O. Løseth, 2009, Investigating the exploration potential for 3D CSEM using a calibration survey over the Troll Field: First Break, **27**, no. 6, 67–75.

Harris, P. E., Z. Du, L. MacGregor, W. Olsen, R. Shu, and R. Cooper, 2009, Joint interpretation of seismic and CSEM data using well log constraints: an example from the Luva Field: First Break, **27**, no. 4, 73–81.

Hoversten, G. M., F. Cassassuce, E. Gasperikova, G. A. Newman, J. Chen, Y. Rubin, Z. Hou, and D. Vasco, 2006, Direct reservoir parameter estimation using joint inversion of marine seismic AVA and CSEM data: Geophysics, **71**, no. 3, C1–C3, http://dx.doi.org/10.1190/1.2194510.

Mikkelsen, J. K., T. Norheim, and S. I. Sagatun, 2005, The Troll story, 2005: OTC paper 17108.

Morten, J. P., F. Roth, D. Timko, C. Pacurar, A. K. Nguyen, and P. A. Olsen, 2011, 3D reservoir characterization of a North Sea oil field using quantitative seismic and CSEM interpretation: 81st Annual International Meeting, SEG, Expanded Abstracts, 1903–1907.

Zach, J. J., A. K. Bjørke, T. Støren, and F. Maaø, 2008, 3D inversion of marine CSEM data using a fast finite-difference time-domain forward code and approximate hessian-based optimization: 78th Annual International Meeting, SEG, Expanded Abstracts, 614–618.

Acknowledgment: We acknowledge the Troll partners (Statoil, Petoro, Shell, ConocoPhillips, and Total) for permission to publish these results, and the Troll petroleum technology group at Statoil for contributing to the validation.

Corresponding author: jpmorten@emgs.com